

## Thermal Hydraulic Study of Steam Generator of PGSFR

J. Hong<sup>1</sup>, S. Ryu<sup>1</sup>, T.-H. Lee<sup>1</sup>

<sup>1</sup>Korea Atomic Energy Research Institute (KAERI), Daejeon, Korea

*E-mail contact of main author: hong@kaeri.re.kr*

**Abstract.** In Prototype Gen-IV Sodium-cooled Fast Reactor (PGSFR), integral once-through type, counter-flow shell-and-tube heat exchanger with straight vertical tubes was adopted for steam generators. Reliable operation of the steam generators has been a key issue through operating experience of foreign sodium-cooled fast reactors because it is one of the most important components deciding the plant availability and reliability. Non-uniformity in sodium flow and temperature distributions might cause mechanical integrity problems such as tube buckling and tube-to-tube sheet junction failure in straight tubes. This work reports thermal hydraulic study on the sodium flow at the inlet plenum and the temperature distribution in the sodium-side of the PGSFR steam generator based on multidimensional numerical analysis. Optimization of porosity of distributors for achieving circumferentially uniform flow at the inlet plenum was carried out with the STAR-CCM+ CFD package. Then, the multidimensional sodium temperature distribution at tube bundle region was also calculated. Iterative calculations between the STAR-CCM+ and 1-D in-house code (HSGSA) were successfully conducted to acquire the radial and axial sodium temperature distributions under normal operation condition. The thermal hydraulic analysis results will be provided as input data to evaluate the mechanical structure integrity of the steam generator of the PGSFR.

**Key Words:** Sodium-cooled Fast Reactor, Steam Generator, Thermal Hydraulic Analysis.

### 1. Introduction

According to the long-term fast reactor development plan of the Korean government, the Prototype Generation-VI Sodium-cooled Fast Reactor (PGSFR) will be constructed by 2028 [1]. In the 150-MWe Korean prototype SFR, integral once-through type, counter-flow shell-and-tube heat exchanger with straight vertical tubes was adopted for steam generators. Reliable operation of the steam generators has been a key issue through operating experience of foreign sodium-cooled fast reactors because it is one of the most important components deciding the plant availability and reliability. An experimental test for the steam generator will be completed by 2021 to validate a design code and demonstrate the heat transfer performance and reliability. In this work, prior to the test, a computational simulation was carried out to examine the performance of the steam generator numerically and optimize the design parameters.

The temperature differences between parts of the large scale steam generator during operation have to be carefully estimated because it has a number of long and straight tubes. Non-uniformity in sodium flow and temperature distributions might cause mechanical integrity problems such as tube buckling and tube-to-tube sheet junction failure in the straight tubes. According to previous studies [2-5], the flow distribution in the inlet plenum of the sodium-heated steam generator was assessed, and proper flow distributors were designed to make uniform sodium flow distribution. The temperature distributions at the tube bundle region under normal operation and plugged tube conditions were also evaluated to figure out thermal

expansion mismatch between tubes. In India, a model steam generator was tested in the Steam Generator Test Facility (SGTF) to validate the thermal hydraulic and mechanical designs [6].

This work reports thermal hydraulic study on the sodium flow at the inlet plenum and the temperature distribution in the sodium-side of the PGSFR steam generator based on multidimensional numerical analysis. Optimization of porosity of flow distributors for achieving circumferentially uniform flow at the inlet plenum is carried out with the STAR-CCM+ CFD package. Then, the multidimensional sodium temperature distribution at tube bundle region is also acquired by iterative calculation between an in-house design code and the STAR-CCM+ CFD package.

## 2. Analysis of Sodium Inlet Flow Distribution

### 2.1. Domain of Analysis

In order to determine a porosity of the flow distributors at the inlet plenum, a three-dimensional flow part of the inlet plenum was analyzed as an analysis domain (*FIG. 1*). Sodium enters the inlet plenum through the sodium inlet nozzle and flows upwards in an annular space where the two flow distributors exist. Circumferential flow imbalance caused by the sodium introduced from one side is mitigated by the flow distributors, which leads to uniform flow distribution at tube bundle entrance region. For efficient calculation, flow distributors, tube support plates, and tube bundle region were treated as porous regions. A polyhedral mesh with prism layer cells was generated on the geometric domains with a base size of 3 cm, which was selected through a mesh dependency study comparing radial velocity profiles of 2.5, 3, and 5 cm cases. The number of cells was about 1.13 million.

### 2.2. Computational Analysis

Numerical simulations were carried out using commercial computational fluid dynamic package, STAR-CCM+ V11.02.009. Flow analysis model was only employed but heat transfer was not taken into account. The SST (Shear Stress Transport)  $k-\omega$  model was adopted as the turbulence model based on a previous study comparing experimental results and numerical results of the inlet plenum [3]. Mass flow inlet and pressure outlet were applied as

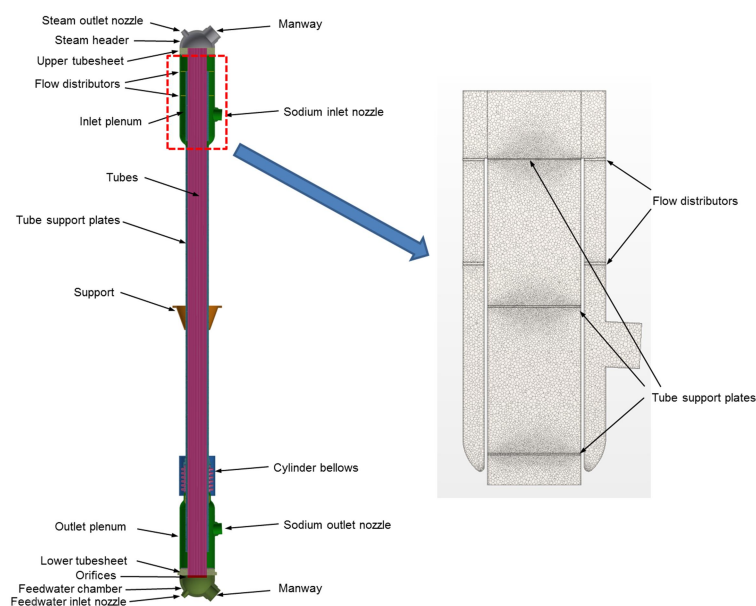


*FIG. 1. Three-dimensional analysis domain and mesh of inlet plenum.*

TABLE I: PRESSURE DROP MODELS FOR POROUS REGIONS.

Porous region	Pressure drop	Nomenclature
Flow distributor or tube support plates [7]	$\Delta p = 0.8 \left[ 0.707(1-P)^{0.375} + 1 - P \right]^2 \left( \frac{1}{P^2} \right) \cdot \frac{1}{2} \rho u^2$	$p$ : pressure $P$ : porosity $\rho$ : sodium density $u$ : sodium velocity
Cross flow in tube bundle [8]	Zhukauskas $\Delta p = Nf\chi \cdot \frac{1}{2} \rho \left( \frac{S_T}{S_T - D} \right)^2 u^2$	$N$ : tube rows $f$ : friction factor $\chi$ : correction factor $S_T$ : tube pitch $D$ : tube outer diameter
Parallel flow in tube bundle [8]	$\Delta p = f \frac{l}{D_h} \cdot \frac{1}{2} \rho u^2$	$D_h$ : hydraulic diameter $l$ : tube length

boundary conditions at inlet and outlet, respectively. Porous inertial resistances of each porous region were acquired with pressure drop models as shown in TABLE I. Parametric study with the porosity of the flow distributors ranging from 20 to 100% was conducted to make uniform flow at the tube bundle entrance and minimize the pressure drop at the distributor devices.

### 2.3. Computational Results and Discussion

FIGS. 2 and 3 show sodium velocity fields during normal operation at the porosity of the flow distributor ranging 45 – 100%. As shown in FIG. 2, at porosity = 100% (without flow distributor), the sodium introduced from the inlet nozzle flowed upwards through the annular space, and enters the tube bundle unevenly at the top of the inlet plenum. The uniformity of the sodium flow at the tube bundle entrance was effectively improved as the porosity decreased. It was shown that at porosity = 45%, a uniform flow was made at the window of the tube bundle entrance. Sodium velocity fields in a horizontal section which is located 5 cm above the window bottom were also obtained at various porosities (FIG. 3). As the porosity of the flow distributor decreased to 45%, circumferentially uniform flow was achieved. Radial velocity profiles along the window height at various angles were analyzed (FIG. 4). As the porosity changed from 100% to 45%, the differences between the radial velocity profiles obtained from various angles were reduced. At porosity = 45%, radial velocities along the height at various angles had a similar trend and decreased with the height. As the sodium flow distribution became circumferentially uniform, the maximum radial velocity was also decreased.

A non-uniformity index ( $NUI$ ) to quantify the non-uniformity of the sodium flow at the tube bundle entrance was defined as EQ (1).

$$NUI = \frac{\sqrt{\sum_s (u_r - \bar{u}_r)^2 / N}}{\bar{u}_r}, \quad (1)$$

where,  $u_r$ ,  $\bar{u}_r$ , and  $N$  are the radial velocity on the window surface of the tube bundle entrance, the surface average of  $u_r$ , and the number of data points, respectively. As the flow distribution becomes uniform on the analysis surface, the  $NUI$  value decreases. As the porosity decreased, the  $NUI$  value decreased but the reduced extent was gradually diminished (FIG. 5a). However, the total pressure drop at the inlet plenum abruptly increased at the porosity range of less than about 45% (FIG. 5b). In conclusion, the optimal porosity for the flow distributors which makes the uniform flow distribution and minimizes the pressure drop was evaluated to be about 45%.

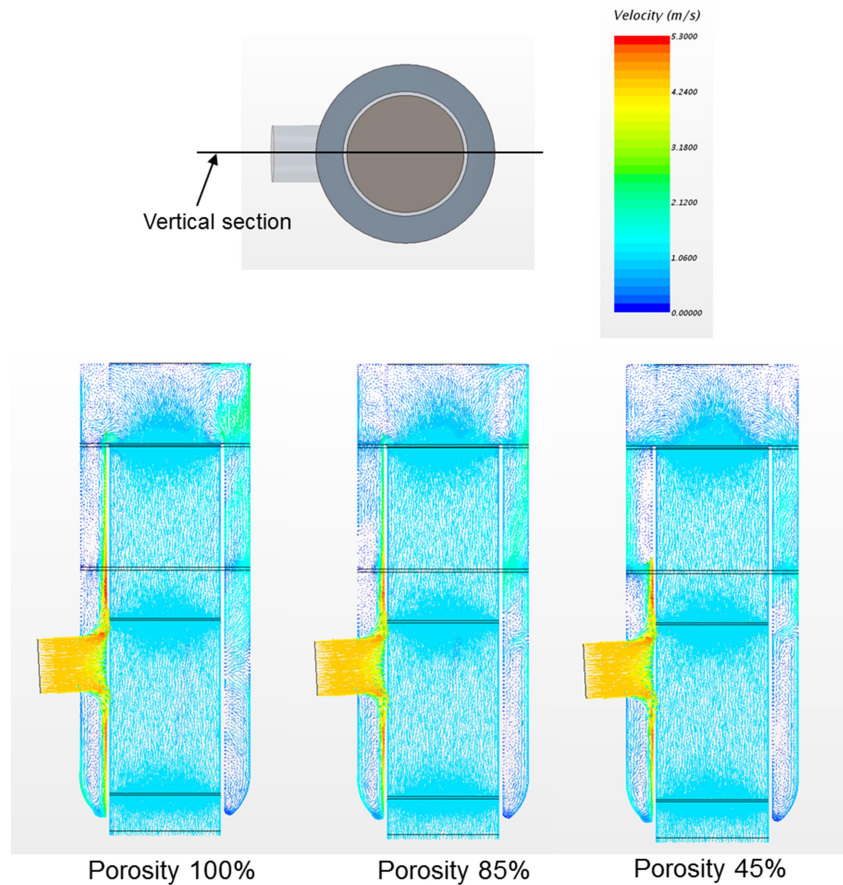


FIG. 2. Sodium velocity fields in a vertical section with respect to porosity of flow distributor.

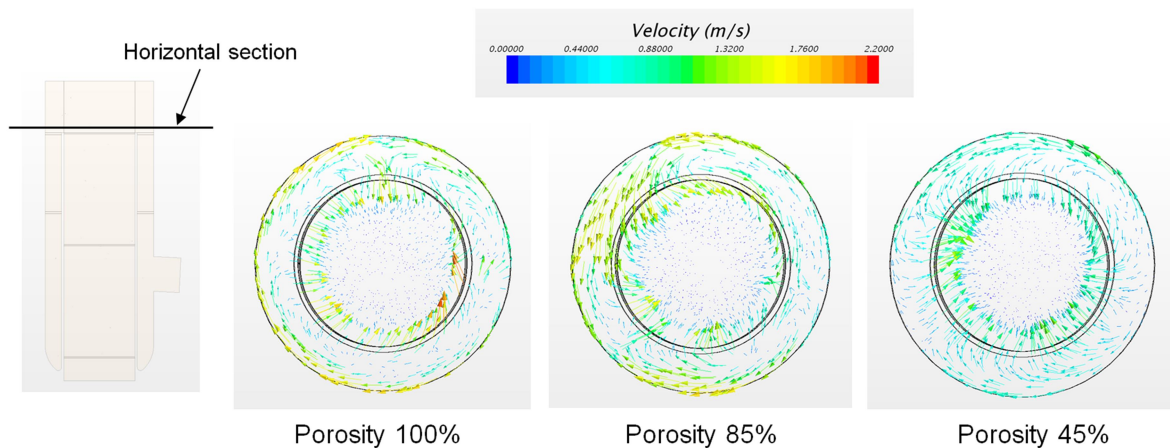


FIG. 3. Sodium velocity fields in a horizontal section with respect to porosity of flow distributor.

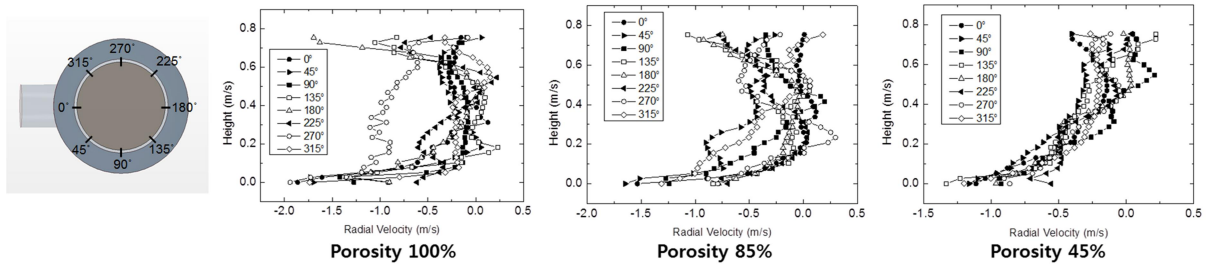


FIG. 4. Radial velocity profiles at tube bundle entrance region.

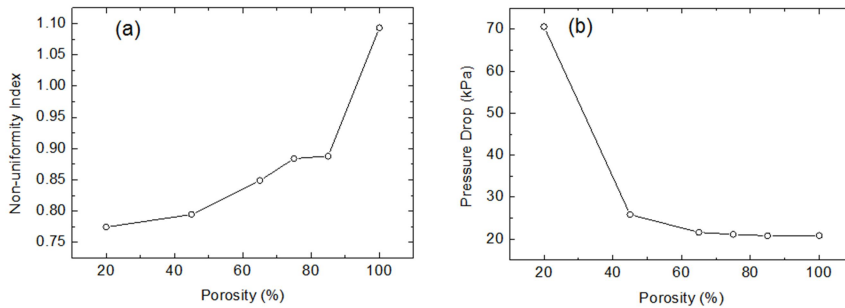


FIG. 5. (a) Non-uniformity index and (b) pressure drop with respect to porosity of flow distributor.

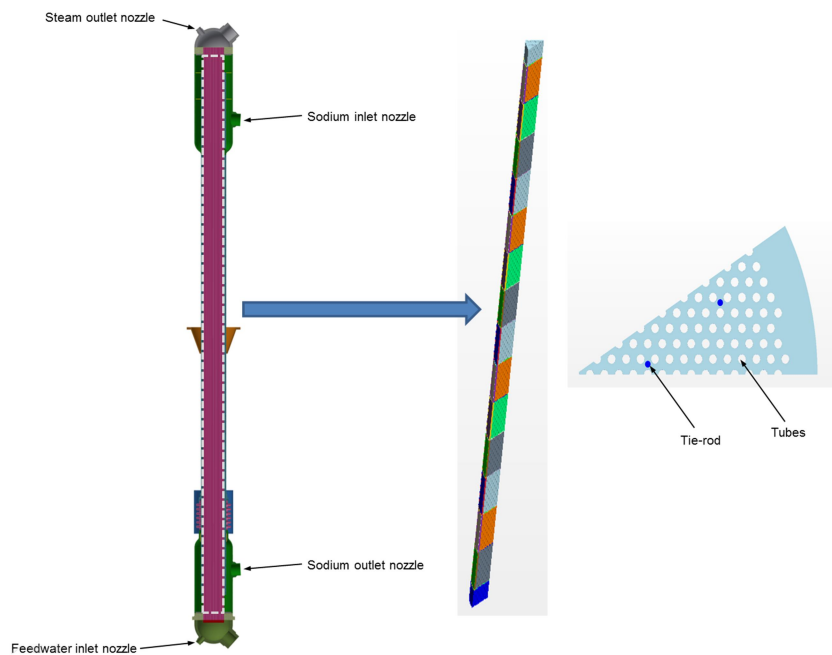


FIG. 6. Three-dimensional analysis domain of tube bundle region.

### 3. Analysis of Sodium Temperature Distribution at Tube Bundle

#### 3.1. Domain of Analysis

A 30° sector domain of the tube bundle region in the steam generator was analyzed to acquire the axial and radial sodium temperature distributions (FIG. 6). The hot sodium circumferentially enters the top of the tube bundle and flows downwards. Fifteen tube support plates which are located at equidistant intervals along the tube hold the tubes and help to make the flow uniform. The sodium transfers heat to the tubes, cools down, and exits radially

at the bottom of the tube bundle. A polyhedral mesh with prism layer cells was employed with a base size of 5 mm, which was selected through a mesh dependency study comparing radial temperature profiles of 3, 5, 10, and 20 mm cases. The number of cells was about 19 million.

### 3.2. HSGSA Code

HSGSA is one-dimensional fortran code used for thermal sizing of the steam generator. It was developed for the design and performance analysis of the shell-and-tube type steam generator with straight tube arrangement. A single flow channel associated with an individual heat transfer tube is basically considered for thermal sizing and then calculation results and design variables regarding heat transfer and pressure drop are extended to a number of tubes. The analysis domain is discretized into tens of control volumes, and heat transfer and pressure losses are calculated in each control volume. Conservation equations for the mass, momentum, and energy balance for both the shell- and tube-sides fluid flow are solved. Various heat transfer correlation for several boiling regimes of the water side and single phase flow of the sodium side are used as shown in TABLE II. The shell- and tube-sides were coupled by analyzing the heat transfer between them. The overall heat transfer coefficient based on the log-mean temperature difference method was determined in each control

TABLE II: HEAT TRANSFER MODELS FOR HSGSA.

Side	Region	Heat transfer model	Nomenclature
Water	Subcooled heating / Super heating	Dittus-Boelter [8] $Nu = 0.23 Re^{0.8} Pr^{0.4}$	<p><math>p</math>: pressure  <math>x</math>: quality  <math>P</math>: tube pitch  <math>D_h</math>: hydraulic diameter</p>
	Nucleate boiling	Thom [9] $q'' = \frac{\exp(2p/8.7)}{(22.7)^2} (T_w - T_{sat})^2$	
	Film boiling	Bishop [10] $Nu = 0.0193 Re^{0.8} Pr^{1.23} \left[ x + (1-x) \frac{\rho_g}{\rho_f} \right]^{0.68} \left( \frac{\rho_g}{\rho_f} \right)^{0.068}$	
Sodium	Single phase	Graber-Rieger [11] $Nu = 0.025 + 6.20 \left( \frac{P}{D_h} \right) + aPe^b$ $a = -0.007 + 0.032 \left( \frac{P}{D_h} \right)$ $b = 0.8 - 0.024 \left( \frac{P}{D_h} \right)$	

volume. The thermal resistances in the heat transfer path such as convection resistances both on the shell- and tube-sides, conduction resistance in the tube wall, and fouling resistances on the wall surfaces of the tube were taken into account.

### 3.3. Computational Analysis

To calculate the sodium temperature distributions and tube temperature profiles, the sodium side was analyzed with STAR-CCM+ V11.02.009 and the water/steam side was estimated with the one-dimensional HSGSA code. An iterative calculation scheme which is similar to the one introduced in the previous Indian study [5] was employed. Initially, the heat flux profiles along each tube wall were obtained by calculating two-phase heat transfer of the water side with the HSGSA code. Those results were applied as heat flux boundary conditions on the tube walls in the STAR-CCM+ simulation. Then, radial temperature distribution obtained from STAR-CCM+ was taken into the input of HSGSA. The inlet and exit sodium temperatures for each tube were calculated and used in the HSGSA to determine the heat flux boundary conditions of each tube for the next sequence. The iterative calculation was conducted until convergence criteria that the sodium exit temperatures of each tube should change within 1% deviation compared to the previous iteration was met. The  $k-\varepsilon$  model was adopted as the turbulence model based on a previous study [5]. A linear velocity profile along the height was roughly assumed as sodium inlet boundary condition based on the radial velocity profiles at the tube bundle entrance region (*FIG. 4*) acquired in the previous flow analysis for the sodium inlet plenum. A pressure outlet was applied as outlet boundary condition. For normal operation, inlet temperature conditions for the sodium and feedwater were set to be 528°C and 240°C, respectively. The tube support plates were treated as porous regions, and the pressure drop model for their porous inertial resistances was displayed in TABLE I. After the iterative calculation converged, the radial and axial sodium temperature distributions and longitudinal tube temperature profiles were obtained from STAR-CCM+ and HSGSA, respectively.

### 3.4. Computational Results and Discussion

As shown in *FIG. 7a*, the fifteen tube support plates made uniform sodium flow distribution at the tube bundle region. In addition, a baffle structure in the periphery of the tube support plate generated recirculation in sodium by-pass flow. The mixing effect by the baffles in the periphery was obviously displayed in a vertical temperature distribution (*FIG. 7b*). The sodium temperature distribution at the tube bundle was relatively uniform in radial because the sodium flow was uniform by the tube support plate. However, the sodium temperature in the periphery was hotter than that in the tube bundle due to the influence of the sodium by-pass. *FIG. 7c* represents typical radial temperature profiles at various elevations. In the top part, the radial temperature difference was approximately 25°C. In the middle part, the temperature difference increased to about 100°C. In the bottom part, relatively uniform temperature distribution in radial was achieved due to the cross flow effect. The horizontal temperature distributions at elevations of 25.3, 12.5, and 0.3 m also showed the similar trend, and the hottest regions in the periphery made the temperature difference even larger (*Fig. 8*).

*FIG. 9a* shows how to number each tube for analysis of average tube temperatures. In order to figure out the radial variation of the tube temperature, the average tube temperatures of the tubes no. 1 ~ 15 were displayed in *FIG. 9b*. As the location of the tube went to the periphery, the average tube temperature increased from 387 to 413°C. Also, the average temperature difference between the central tubes (no. 1 and 2) and the peripheral tubes (no. 15, 29, 41, 51, 60, 67, 72, 75, and 76) was found to be 25°C. Average temperature on outermost surface of

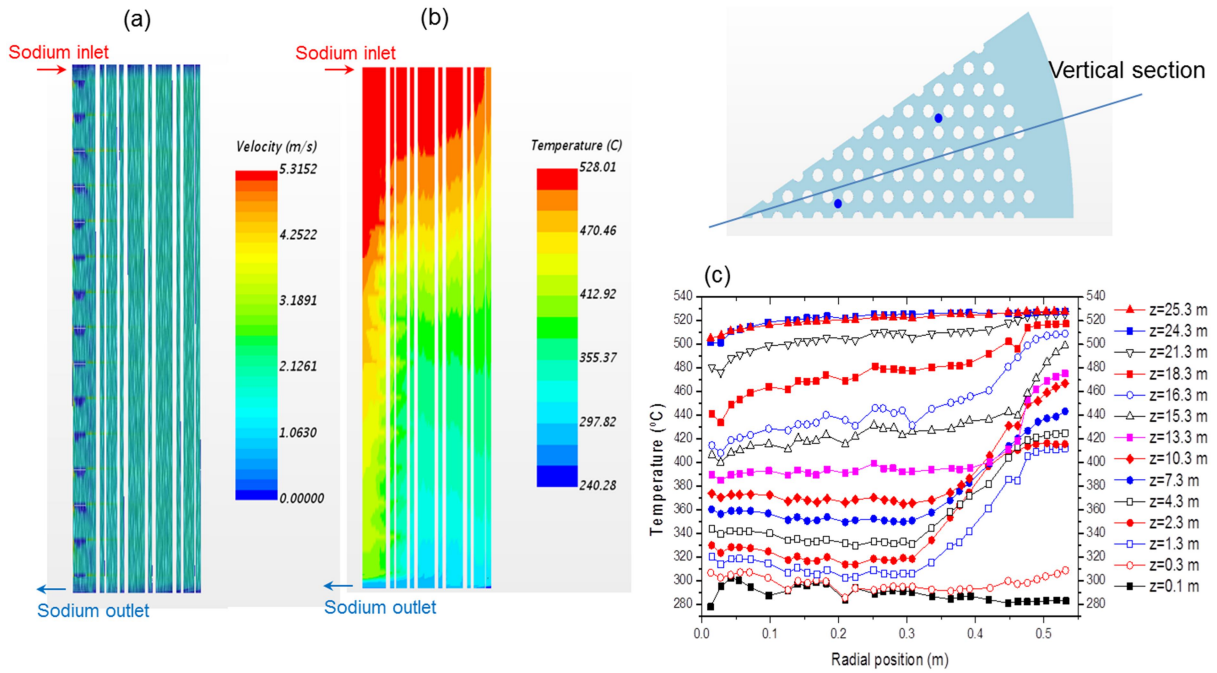


FIG. 7. (a) Flow distribution, (b) temperature distribution, and (c) radial temperature profiles in a vertical section of steam generator.

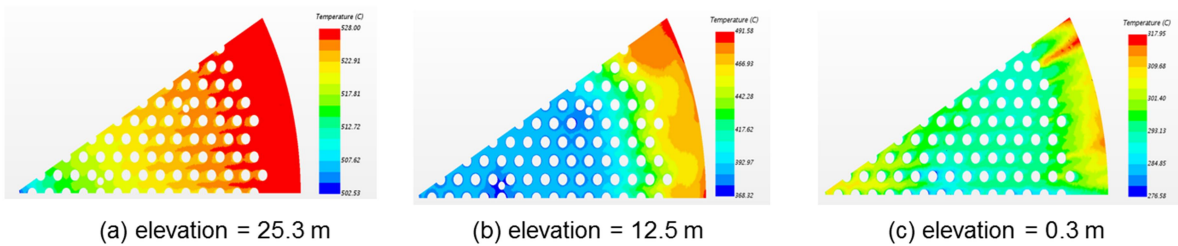


FIG. 8. Temperature distribution in a horizontal section at elevation of 25.3, 12.5, and 0.3 m.

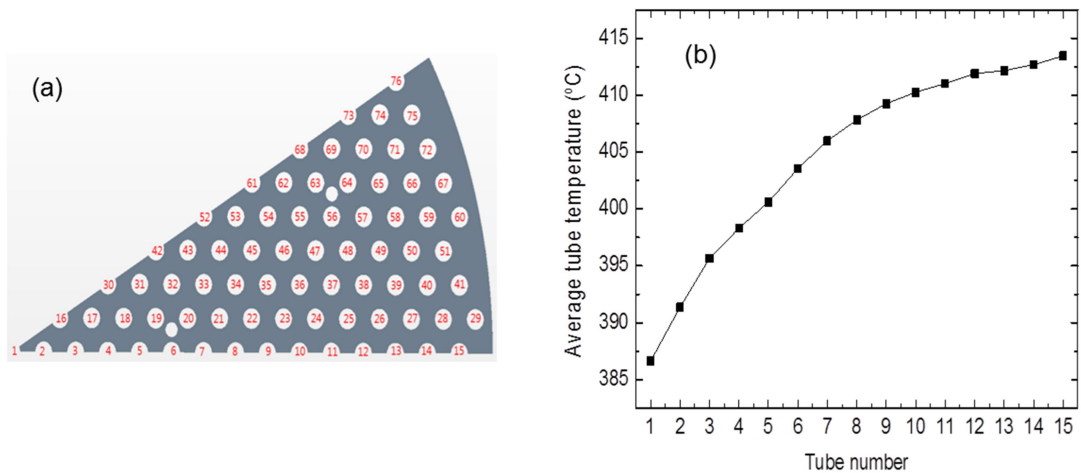


FIG. 9. Analysis of average temperature of each tube; (a) numbering of tubes, (b) average temperature of tubes no. 1~15.

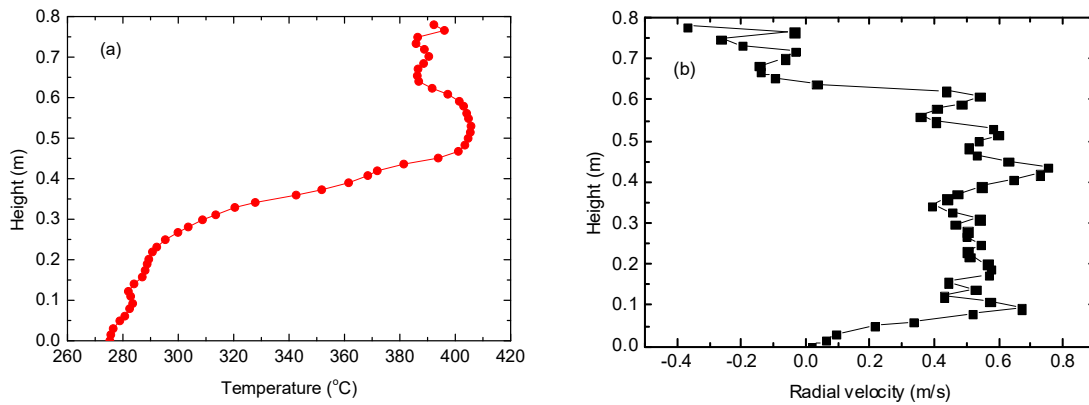


FIG. 10. (a) Sodium temperature and (b) radial velocity profiles along the height at the sodium exit.

the sodium which is relevant to the average temperature of the shell cylinder was 477°C.

Average temperature at the sodium exit was 337°C which was 0.3% higher than 332°C, the estimated value in the one-dimensional analysis by HSGSA. In the radial sodium exit of the bottom, a stratified flow was observed since the peripheral hot sodium flow did not mix well with the central cold sodium flow. FIG. 10a shows the typical sodium temperature profile along the height at the sodium exit. The profile can be divided into three parts, including a hot layer (0.45 ~ 0.78 m), a transition layer (0.25 ~ 0.45 m), and a cold layer (bottom ~ 0.25 m). Maximum temperature difference on the sodium exit surface was 139°C. Fig. 10b displays the typical radial velocity profile along the height at the sodium exit. The hot sodium recirculated in the upper part (0.65 ~ 0.78 m) with inward flow direction. Below the recirculation zone, nearly uniform outward flow was observed, and the magnitude of the radial velocity approached zero in the vicinity of the bottom.

#### 4. Conclusion

Prior to the experimental validation of the PGSFR steam generator, numerical thermal hydraulic analysis was carried out to select the porosity of the flow distributors at the inlet plenum and assess the sodium and tube temperatures during normal operation. The porosity of the flow distributors was determined to be 45%, considering the flow uniformity and pressure drop. During normal operation, the radial temperature difference by peripheral by-pass sodium flow caused the average temperature difference of 25°C between the central tubes and peripheral tubes. In the radial sodium exit, the peripheral hot sodium flow did not mix well with the central cold sodium flow, which led to a thermally stratified flow. The thermal hydraulic analysis under various plugged tube conditions is also in progress. The mechanical structure analysis of the PGSFR steam generator using the results of this work will be carried out.

#### 5. Acknowledgment

This work was supported by the National Research Foundation of Korea (NRF) grant funded by the Korean Government (MSIP). (No. 2012M2A8A2025624)

## 6. References

- [1] Yoo, J., “Status of prototype Gen-IV sodium cooled fast reactor and its perspectives”, Proceedings of Transactions of the Korean Nuclear Society Autumn Mtg., Gyeongju, Korea (2015).
- [2] Kisohara, N., et al., “Temperature and flow distributions in sodium-heated large straight tube steam generator by numerical methods”, Nuclear Technology **164** (2008) 103.
- [3] Patil, L.T., et al., “Distribution of liquid sodium in the inlet plenum of steam generator in a Fast Breeder Reactor”, Nuclear Engineering and Design **240** (2010) 850.
- [4] Khadamakar, H.P., et al., “Flow distribution in the inlet plenum of steam generator”, Nuclear Engineering and Design **241** (2011) 4165.
- [5] Nandakumar, R., et al., “Thermal simulation of sodium heated once through steam generator for a fast reactor”, Int. J. Adv. Eng. Sci. Appl. Math. **4** (2012) 127.
- [6] Vinod, V., et al., “Experimental evaluation of the heat transfer performance of sodium heated once through steam generator”, Nuclear Engineering and Design **273** (2014) 412.
- [7] Idelchik, I.E., Handbook of Hydraulic Resistance, 3rd Edition, Begell House, New York (1996).
- [8] Incropera, F.P. et al., Fundamentals of Heat and Mass Transfer, 4th Edition, John Wiley & Sons, Inc., New York (1996).
- [9] Thom, J.R.S. et al., “Boiling in Subcooled Water During Flow up Heated Tubes or Annuli”, Symposium on Boiling Heat Transfer in Steam Generating Units and Heat Exchangers, London, United Kingdom (1965)
- [10] Bishop, A.A. et al., “Forced Convection Heat Transfer at High Pressures After the Critical Heat Flux”, ASME Paper 65-HT-31 (1965).
- [11] H. Graber et al., “Experimental Study of Heat Transfer to Liquid Metals Flowing In-line through Tube Bundles”, Prog. Heat Mass Transfer **7** (1973) 151.